EDN BNDWLP

Jet Electrical Discharge with a Liquid Plasma-Forming Medium in Interaction with Aluminum

© S.Yu. Petryakov, E.R. Belgibaev, R.R. Kayumov, A.F. Gaisin

Kazan National Research Technical University named after A. N. Tupolev – KAI, Kazan, 420111, Russian Federation

We present the results of an experimental–theoretical study of a jet electrical discharge with a liquid plasma-forming medium interacting with aluminum. The discharge was realized in the "jet anode—aluminum cathode" configuration at atmospheric pressure within the ranges: voltage 0.1–1.1 kV, jet velocity 0.5–0.7 m/s, jet diameter 2 mm, free jet length 15 mm, solution conductivity 0.10–0.12 $\Omega^{-1}\cdot cm^{-1}$, temperature 12–64 °C. High-speed imaging revealed two typical discharge geometries: a longitudinal channel along the jet body and a near-surface conical luminous plume at the "liquid–gas–metal" interface. A threshold transition was identified from an electrochemical regime (≈200 V, intense bubble formation, no discharge) to an impulse plasma regime (≈700 V) with current pulses of 1.0–1.2 A and widths up to 500 μs. Emission spectroscopy showed OH(A–X), N_2^+(B–X), and H I, Na I, N I, Al I lines; electron density was evaluated from Stark broadening of Balmer lines: $\approx 1.76\times10^{16}$ cm^{-3} from Hβ (with instrumental function accounted for) and $\approx 6.64\times10^{15}$ cm^{-3} from Hα. Thermography registered a local maximum of the jet anode temperature near the contact zone of ~64 °C with an exponential decay to room background. The combined electrical, spectral, and thermal diagnostics substantiate operating "windows" for controlled local modification of the oxide film and near-surface layer of aluminum without thermal damage—promising for surface preparation before coatings, adhesive and brazed joints.

Keywords: *jet electrical discharge; liquid plasma-forming medium; aluminum; emission spectroscopy; Stark broadening; electron density; thermography; local surface modification*

Introduction. In recent years, jet low-temperature plasma discharges with a liquid plasma-forming medium have been considered a convenient tool for local surface modification and controlled delivery of reactive species into a confined zone. Their key feature is the dual role of the liquid as both an electrode and a source of plasma-forming components, which ensures rich plasma chemistry at the mobile "gas–liquid–solid" interface. This configuration combines the advantages of gas-discharge technologies (high reactivity, nonequilibrium conditions, controllable energy and charge fluxes) and liquid-phase chemistry (tunable composition, buffering and catalytic functions), enabling fine control of material treatment without aggressive etchants or heavy thermal loads.

For aluminum, the interest is particularly strong. The surface of aluminum alloys is rapidly covered by a dense nanometric oxide film that governs adhesion, wettability, corrosion resistance, and behavior during

soldering, cladding, and coating deposition. While the oxide protects the metal, it also hinders formation of strong joints and uniform functional layers. Traditional preparation routes—mechanical abrasion, alkaline–acid pickling—often cause excessive material removal, result variability, and environmental constraints. A jet electrical discharge with a liquid medium offers a local, metered, and typically more environmentally benign modification of the oxide and the near-surface layer, with the ability to change their structure and chemistry selectively.

The physics of interaction of a jet discharge with aluminum is governed by the dynamics of the interfacial region and competing transports: ion–electron, thermal, vapor–aerosol mass transfer, and reaction–diffusion processes in the oxide. Discharge types and burning forms, fluxes and composition of active species to the substrate are determined not only by electrical parameters (power/voltage, current, frequency, pulsing) but also by jet hydrogas dynamics (flow rate, velocity, nozzle diameter, interelectrode gap) and liquid properties (conductivity, pH, volatility, surface tension). For aluminum, high thermal conductivity and a comparatively low melting temperature demand limited thermal impact and a stable non-destructive operating regime. Despite progress, several aluminum-specific issues remain open: mapping the stability domains of the jet discharge versus ambient pressure and gas composition; conditions for transitions between diffuse and constricted/filamentary forms; quantitative roles of bubble formation and electrocapillary effects in oxide evolution; and the contribution of aerosol/vapor fluxes to material transfer.

For engineering use, reproducible operating “windows” are needed that link-controlled changes in morphology and oxide chemistry to target properties—adhesion, wettability, corrosion resistance, and near-surface mechanical integrity—while minimizing thermal load and avoiding defects such as local melting and recrystallization. Modern diagnostics enable a comprehensive approach: V–A characteristics and high-speed imaging reveal discharge dynamics and characteristic times; optical emission spectroscopy and IR thermography expose active-species composition and thermal fluxes; profilometry and electron microscopy evaluate microrelief; contact-angle measurements assess wettability; micro/nano-hardness and electrochemical tests characterize corrosion resistance of aluminum and its alloys. Numerical modeling that couples electrical, fluid, and plasma-chemical subsystems complements the experiments and supports transfer to other alloys and geometries. The engineering relevance spans aerospace and transport, additive and thin-film manufacturing, and pre-bond surface preparation. The jet’s locality and choice of liquid facilitate integration into robotic lines and selective repair of complex parts. Accordingly, this work aims to build operating maps and recommendations that predictably control aluminum oxide and the near-surface layer as a function of electrical/hydrodynamic parameters and liquid composition.

Experimental Setup. Ignition and sustainment of the jet electrical discharge with a liquid plasma-forming medium on an aluminum plate surface were carried out on a laboratory rig where the liquid jet served as an anode and the aluminum plate as a cathode (Fig. 1). An Al-Mg alloy plate (AMts-40 grade) was used as the metallic cathode; a 3 wt% NaCl aqueous solution prepared with purified tap water served as the jet anode. Before operation, a positive potential was applied to the jet nozzle; the jet was directed to the aluminum plate mounted in an electrolytic cell filled with the working solution, while a negative potential was applied to the plate. To stabilize operation, the bath was thermostated with a refrigerated recirculating chiller; solution renewal was provided by a closed-loop feed/return circuit with a coarse filter.

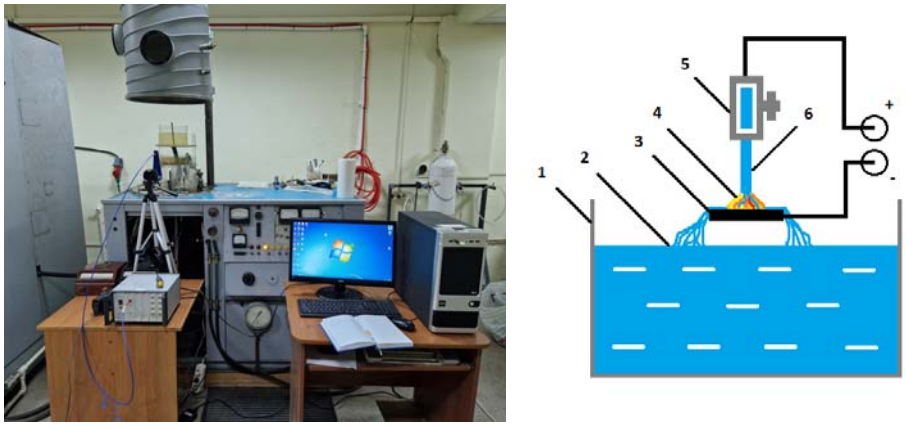

a b

Fig. 1. Photograph of the experimental setup (a) and functional diagram of the discharge chamber (b) used to sustain a jet discharge with a liquid medium at the aluminum surface.
Legend:
1 — electrolytic cell; 2 — electrolyte; 3 — aluminum plate; 4 — discharge zone;
5 — nozzle/flow regulator; 6 — liquid jet

Vapors and discharge products were removed by a fixed hood and fan. All live parts and housings were grounded. A high-voltage power supply (up to 40 kW, up to 4 kV, nominal current up to 10 A) powered the discharge and auxiliary diagnostics. High- and low-voltage regulated modules allowed setting the required voltage/current ranges and feeding diagnostic equipment. Instantaneous voltage and current were displayed on analog meters and mirrored to a control PC. Experiments were performed at: voltage U = 0.1–1.1 kV; pressure $p \approx 1\times10^5$ Pa (atmospheric); jet velocity v_a = 0.5–0.7 m/s; jet diameter d = 2 mm; free jet length l = 15 mm; solution conductivity σ = 0.10–0.12 $\Omega^{-1}\cdot cm^{-1}$; solution temperature T = 12–64 °C. High-speed imaging of the plume and plasma structures used a Casio EX-F1 camera at 600 and 1200 fps positioned ~300 mm

from the discharge; data were captured and processed on a PC (HX Link, Movavi Video Editor 14 Plus). Temperature fields on the cathode surface and in the jet region were recorded by a FLIR A6500sc (640×512 detector, 3.6–4.9 μm), calibrated with a multiband pyrometer to mitigate emissivity changes due to oxide formation; thermal data were processed in ALTAIR v5.91.010. Current/voltage pulsations were measured by digital oscilloscopes (GDS-806S, GOS-6030); a photodiode optical sensor provided timing of optical events for synchronization. Plasma emission was measured with a fiber-optic spectrometer (PLASUS EC 150201 MC) for 195–1105 nm, with instrumental function calibrated by a SIRSh-6-100 lamp. The instrumental FWHM of the narrowest lines was $\Delta\lambda\_G \approx 1$ nm. Spectra were compared with the NIST database; rotational/vibrational temperatures were estimated using LIFBASE and SPECAIR 2.2.0.0.

Discussion of Results. A free liquid jet impinged on the aluminum surface to initiate the discharge. High-speed imaging (Fig. 2) shows two typical geometries: a longitudinal channel stretched along the jet axis and a near-surface conical luminous plume at the jet–aluminum contact.

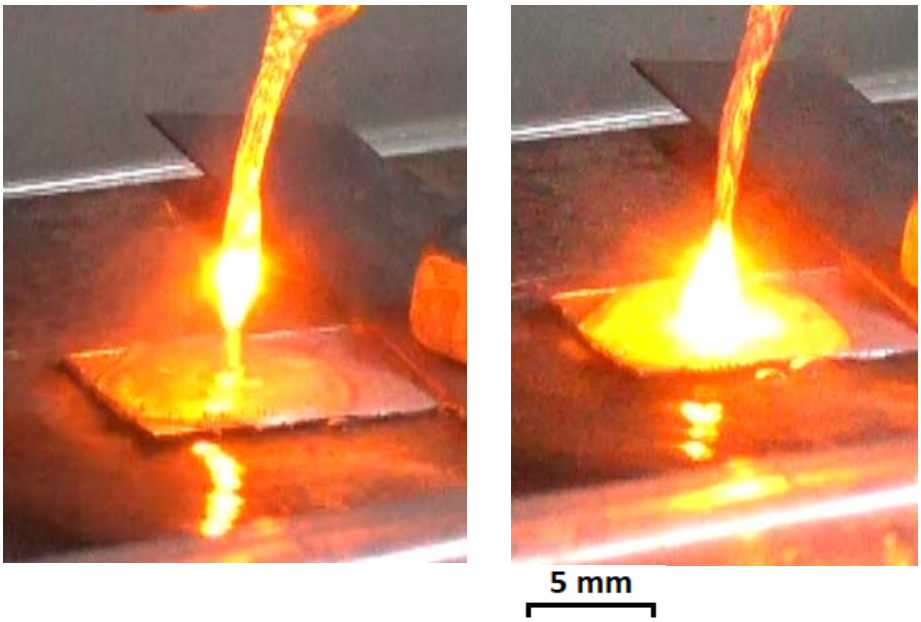

Fig. 2. Photographs of the discharge between a jet anode and aluminum cathode at $U = 700$ V, $I = 1.2$ A, $p = 10^5$ Pa; (a) $v\_a = 0.5$ m/s; (b) $v\_a = 0.7$ m/s

At ~200 V, electrochemical processes dominate: intense bubble formation and evaporation, with a quasi-stationary conduction current around 0.8 A (Fig. 3, a) and no gas-discharge channel. Raising the voltage to ~700 V produces a thin vapor–gas sheath due to Joule heating and evaporation, which enhances the local electric field at the “liquid–gas–metal” boundary

and triggers micro-breakdowns. The current becomes pulsed, with packets of pulses of 1.0–1.2 A and widths up to 500 μs (Fig. 3, b). Flow regime plays a key role: at lower velocity, dripping/jetting forms inter-drop gaps where channels ignite; at higher velocity the maximum field shifts to the cathode surface and a stable near-surface conical plume is formed. The observed yellow tint corresponds to Na I resonance lines (~589 nm), consistent with the 3 % NaCl solution.

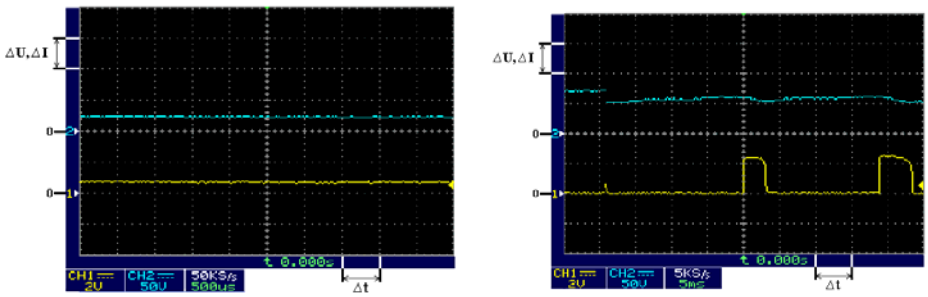

a b

Fig. 3. Oscillograms of current/voltage pulsations for the same discharge: $\Delta U = 500V$, $\Delta I = 2A$, $\Delta t = 500\,mcs$

An emission spectrum of the plasma (Fig. 4) shows OH(A–X) bands, N_2^+(B–X) bands, and atomic lines of H I, Na I, N I, and Al I. Instrumental broadening was evaluated from an optically thin Al I line at 669.7 nm; the minimal FWHM ($\Delta\lambda\_G$) was ~1 nm.

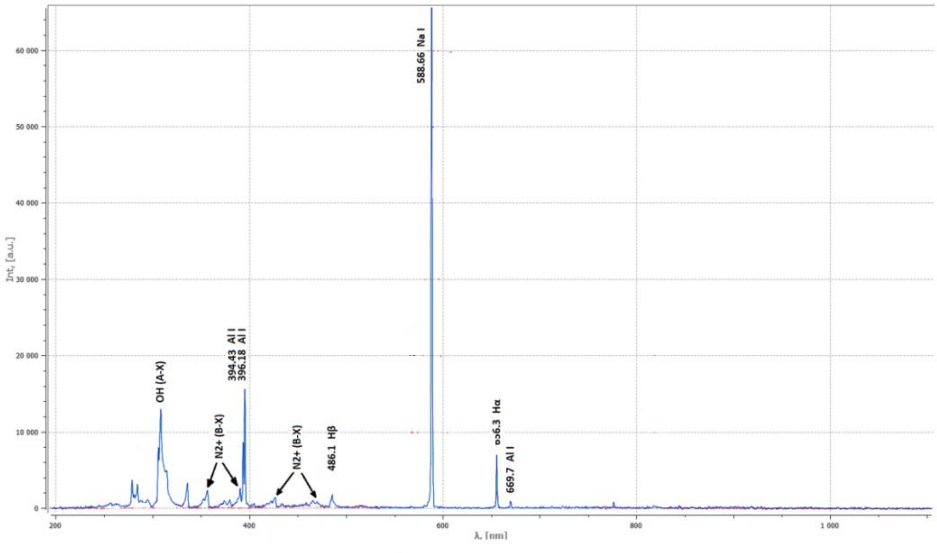

Fig. 4. Emission spectrum of the plasma between the jet anode and aluminum cathode with assigned lines

Measured FWHM (Δλ_*F*) was fitted by a Voigt profile, and the Lorentzian component (Δλ_*L*) was obtained from the standard relation to separate pressure/Stark broadening from instrumental width:

$$\Delta\lambda_F \approx 0,5346 \cdot \Delta\lambda_L + \sqrt{0,2166 \cdot \Delta\lambda_L^2 + \Delta\lambda_G^2}.$$

Electron density *n_e* was then evaluated from Stark broadening of Balmer lines using temperature-dependent coefficients (Kasabov) (Table 1). For *H*β, Δλ_*F* = 1.983 nm gave Δλ_*L* = 1.1452 nm, and *n_e* ≈ 1.76×10^{16} cm^{-3}. For *H*α, Δλ_*F* = 1.054 nm gave Δλ_*L* = 0.099 nm and *n_e* ≈ ≈ 6.64×10^{15} cm^{-3}, consistent with stronger self-absorption of *H*α (Table 2):

$$n_e = 10^{13} \left(\Delta\lambda_L\right)^{\frac{3}{2}} \left[C_0\left(T\right) + \sum_{n=1}^{m} C_n\left(T\right) \left(ln\Delta\lambda_L\right)^n \right].$$

Table 1. Coefficients for calculating the electron density from the emission spectra of hydrogen Balmer-series lines [17]

Coefficient C_n	*H*α	*H*β
C_0	671.4	36.56
C_1	–227.5	–1.45
C_2	44.72	–0.109
C_3	–2.325	0.005

Table 2. Electron density derived from Hα and Hβ lines

Balmer line	*H*α	*H*β
Voigt FWHM, nm	1.054	1.983
Lorentzian FWHM (after deconvolution), nm	0.099	1.1452
Electron density, cm^{-3}	6.64·10^{15}	1.76·10^{16}

Thermograms of the jet anode surface during discharge operation show a local maximum near the contact zone with the aluminum cathode at approximately 64 °C, with an exponential decay toward room temperature outside the plasma zone (Fig. 5). This corresponds to localized Joule heating and heat release in the near-surface vapor–gas sheath, with efficient removal by convection and evaporation. Isotherm asymmetry along the jet axis and 2–3 °C oscillations correlate with dripping transitions and discharge pulsations. The temperatures remain far below aluminum melting yet are sufficient for controlled modification of the oxide and the near-surface layer.

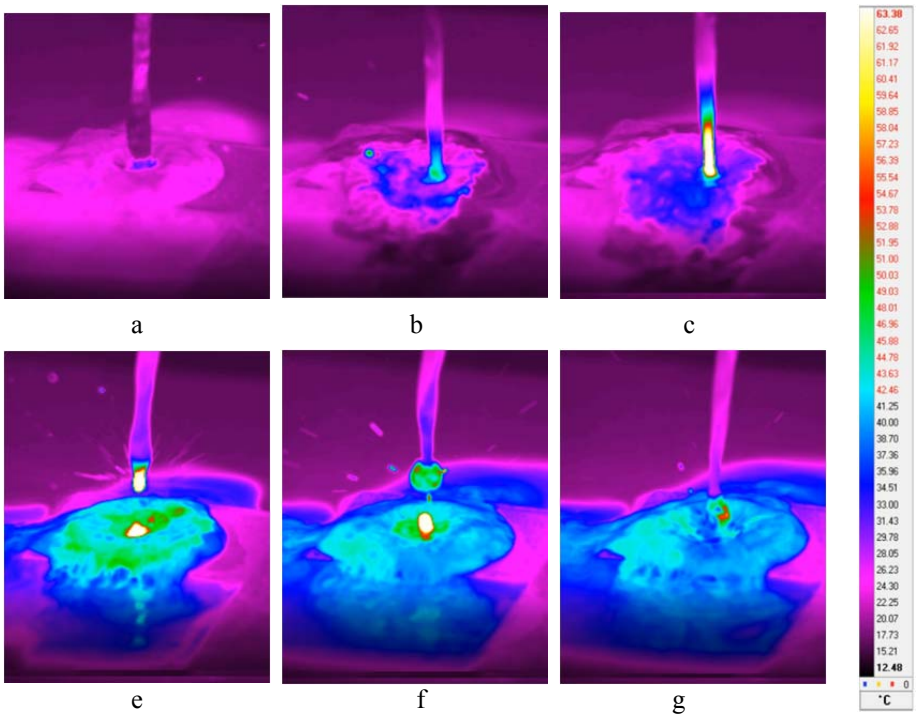

Fig. 5. Thermograms of the jet anode surface during the discharge

Conclusion. The jet electrical discharge with a liquid plasma-forming medium interacting with aluminum is stably realized within $U = 0.1–1.1$ kV, $p \approx 10^5$ Pa, $v\_a = 0.5–0.7$ m/s, $d = 2$ mm, $l = 15$ mm, $\sigma = 0.10–0.12$ $\Omega^{-1}\cdot cm^{-1}$, $T = 12–64$ °C. Two typical geometries are observed: a longitudinal channel along the jet and a near-surface conical plume at the "jet–aluminum" interface. A threshold transition from an electrochemical regime at ~200 V (bubble formation, ~0.8 A quasi-stationary current, no discharge) to an impulse plasma regime at ~700 V (current pulses 1.0–1.2 A, up to 500 μs) is governed by the growth–breakdown–collapse–recovery cycle of a vapor–gas sheath. Emission spectroscopy reveals a mixed plasma composition (OH, N_2^+, H, Na, N, Al), with electron density derived from Balmer Stark broadening at ~1.76×10^{16} cm^{-3} ($H\beta$) and ~6.64×10^{15} cm^{-3} ($H\alpha$). Thermography confirms a contact-zone maximum of ~64 °C, well below aluminum melting, enabling controlled modification of the oxide film and the near-surface layer without thermal damage. These operating windows and diagnostics support local surface preparation prior to coatings and adhesive/brazed joints and integration into robotic selective-repair processes.

Acknowledgment

This research was supported by the Russian Science Foundation, Project No. 25-29-20147 (https://rscf.ru/project/25-29-20147/).

REFERENCES

[1] Gaisin A.F., Kashapov N.F. Investigation of physical processes in the gas-discharge zone between liquid electrodes. *Journal of Applied Mechanics and Technical Physics*, 2018, vol. 59, no. 4, pp. 19–22. doi: 10.1134/S002189441804003X.

[2] Gaisin A.F., Son E.E., Efimov A.V., Gil'mutdinov A.Kh., Kazhapov N.F. Spectral diagnostics of plasma discharge between a metal cathode and liquid anode. *High Temperature*, 2017, vol. 55, pp. 457–460. doi: 10.1134/S0018151X17030087.

[3] Kashapov N., Kashapov R., Kashapov L. Influence of the electrolytic cathode temperature on the self-sustaining mechanism of plasma-electrolyte discharge. *Journal of Physics D: Applied Physics*, 2018, vol. 51, 494003. doi: 10.1088/1361-6463/aae334.

[4] Bruggeman P., Kushner M. J., Locke B.R., *et al.* Plasma–liquid interactions: a review and roadmap. *Plasma Sources Science and Technology*, 2016, vol. 25, 053002. doi: 10.1088/0963-0252/25/5/053002.

[5] Akishev Y.S., Grushin M.E., Karal'nik V.B., Monich A.E., Pan'kin M.V., Trushkin N.I., Kholodenko V.P., Chugunov V.A., Zhirkova N.A., Irkhina I.A., Kobzev E.N. Creation of nonequilibrium plasma in gas–liquid heterogeneous media at atmospheric pressure and demonstration of its capabilities for sterilization. *Plasma Physics Reports*, 2006, vol. 32, no. 12, pp. 1142–1152. doi: 10.1134/S1063780X06120087.

[6] Barinov Yu. A., Shkol'nik S. M. Discharge with a liquid non-metallic cathode (tap water) in an air flow at atmospheric pressure. *Zhurnal Tekhnicheskoi Fiziki* (Journal of Technical Physics), 2016, vol. 86, no. 11, pp. 155–158. doi: 10.21883/jtf.2016.11.43833.1833.

[7] Samitova G.T., Gaisin A.F., Mustafin T.B., Gaisin A.F., Son E.E., Veselev D.A., Gaisin F.M. Some features of a multichannel discharge in a tube at atmospheric pressure. *High Temperature*, 2011, vol. 49, no. 5, pp. 788–792. doi: 10.1134/S0018151X11050208.

[8] Sirotkin N.A., Titov V.A. Experimental study of liquid-cathode heating and transfer of its components into the gas phase under a DC discharge. *Prikladnaya Fizika*, 2016, no. 6, pp. 25–31.

[9] Valiev R.I., Khafizov A.A., Bagautdinova L.N., Gaisin F.M., Basyrov R.Sh., Gaisin Az.F., Gaisin Al.F., Zheltukhin V.S., Son E.E. AC electrical discharges in a gas–liquid medium of sodium chloride solution at atmospheric pressure. *High Temperature*, 2021, vol. 59, no. 4, pp. 634–637. doi: 10.31857/S0040364421040219.

[10] Gaisin Al.F., Gaisin F.M., Zheltukhin V.S., Son E.E. High-frequency discharge with a jet electrolytic electrode. *Plasma Physics Reports*, 2022, vol. 48, no. 1, pp. 71–78. doi: 10.31857/S1063780X22010061.

[11] Gaisin A.F., Son E.E., Petryakov S.Yu. Radio-frequency capacitive discharge with flowing liquid electrodes at reduced pressure. *Plasma Physics Reports*, 2017, vol. 43, no. 7, pp. 625–633. doi: 10.1134/S1063780X17070054.

[12] Averin K.A., Lebedev Yu.A., Shakhatov V.A. Some results of investigating a microwave discharge in liquid heavy hydrocarbons. *Prikladnaya Fizika*, 2016, no. 2, pp. 41–45.

[13] Gaisin A.F., Kayumov R.R., Kuputdinova A.I., Mardanov R.R. Plasma–liquid recycling of metal powder for 3D printing. *Fizika i Khimiya Obrabotki Materialov*, 2023, no. 1, pp. 37–44. doi: 10.30791/0015-3214-2023-1-37-44.

[14] Gaisin A.F., Gilmutdinov A.Kh. Electrolyte-plasma treatment of a part manufactured by additive technology. *Fizika i Khimiya Obrabotki Materialov*, 2020, no. 2, pp. 28–34. doi: 10.30791/0015-3214-2020-2-28-34.
[15] Gaisin A.F., Gilmutdinov A.Kh., Mirkhanov D.N. Electrolyte-plasma treatment of the surface of a part manufactured using additive technology. *Metal Science and Heat Treatment*, 2018, vol. 60, pp. 128–132. doi: 10.1007/s11041-018-0250-1.
[16] Petryakov S.Yu., Mirkhanov D.N., Gaisin A.F., Basyrov R.Sh., Kashapov N.F. DC discharge between a metal anode and a liquid non-metallic cathode. *Journal of Applied Mechanics and Technical Physics*, 2022, vol. 63, no. 5, pp. 20–32. doi: 10.1134/S0021894422050029.
[17] Kasabov G.A. *Spectroscopic Tables for Low-Temperature Plasma*. Moscow, Atomizdat Publ., 1973, p. 8. (in Russ.)
[18] Ochkin V.N. *Spectroscopy of Low-Temperature Plasma*. Moscow, Fizmatlit Publ., 2006. (in Russ.)

Petryakov S.Yu., Assistant, Department of Technical Physics, Kazan National Research Technical University named after A.N. Tupolev – KAI. Research interests: gas discharge physics. e-mail: serioga_com@mail.ru

Belgibaev E.R., Assistant Professor, Department of Technical Physics, Kazan National Research Technical University named after A.N. Tupolev – KAI. His research interests include gas discharge physics. e-mail: erbelgibaev@kai.ru

Kayumov R.R., PhD (Eng.), Associate Professor, Department of Technical Physics, Kazan National Research Technical University named after A.N. Tupolev – KAI. Research interests: gas discharge physics. e-mail: rushan_250189033@mail.ru

Gaisin A.F., Dr. Sc. (Eng.), Associate Professor in Plasma Physics; Head of the Department of Technical Physics, Kazan National Research Technical University named after A.N. Tupolev – KAI. Research interests: gas discharge physics.
e-mail: almaz87@mail.ru